The dynamics of cavity clusters in ultrasonic (vibratory) cavitation erosion

Hansson, I.; Mørch, Knud Aage

Published in:
Journal of Applied Physics

Link to article, DOI:
10.1063/1.328335

Publication date:
1980

Document Version
Publisher's PDF, also known as Version of record

The dynamics of cavity clusters in ultrasonic (vibratory) cavitation erosion

I. Hansson and K. A. Mørch
Laboratory of Applied Physics I, Technical University of Denmark, Building 307, 2800 Lyngby, Denmark

(Received 26 February 1980; accepted for publication 13 May 1980)

The erosion of solids caused by cavitating liquids is a result of the concerted collapse of clusters of cavities. In vibratory cavitation equipment the clusters grow and collapse adjacent to a solid surface and are typically of hemispherical or cylindrical form. In the present paper the collapse process of these clusters is described and the collapse equations are developed and solved. The theoretical results are compared with results from high-speed photography of the clusters and with the initial stages of cavitation erosion on metal specimens. Experimental and theoretical results show that the collapse of a cavity cluster is driven by the ambient pressure and the collapse proceeds from the outer boundary of the cluster towards its center. During the collapse the pressure at the inward-moving cluster boundary increases continuously, and at the cluster center it rises significantly above the ambient pressure. Therefore the collapse velocity of the individual cavities increases towards the cluster center, which explains that the erosion, being caused by the individual cavities, occurs predominantly in this region. Likewise, the pressure increase at the cluster boundary explains why materials of even high strength can be eroded by collapse of cavity clusters at atmospheric ambient pressure.

PACS numbers: 43.25. + y, 47.55.Bx, 81.70. + r, 81.60.Bn

I. INTRODUCTION

One of the expanding areas in the extensive field of surface removal of material or wear is cavitation erosion. The importance of this type of erosion increases with demands for higher flow velocities and use of valves with smaller dimensions and tolerances for more critical flow regulation. The interest in safety considerations in connection with atomic power plants also necessitates more research on cavitation erosion in cooling and sprinkler systems.

Ordinary flow channels are widely used for studying both the cavitation mechanisms and the resulting erosion. They reproduce very well the situation in systems with cavitating flow. However, this type of equipment is expensive and the experiments require long testing time. Therefore vibratory cavitation equipment has been developed for simulation of flow cavitation erosion. This equipment is much faster and easier to use in an industrial test procedure. An ASTM-standard method (G 32-72 [ε])[1] exists for erosion testing of materials by vibratory cavitation. According to this standard the specimen is mounted directly on an ultrasonic horn (moving specimen), but an amendment to this standard will be published shortly, placing the specimen at a controllable distance beneath the horn (stationary specimen).

Until recently, the erosion in cavitating liquids was discussed only on the basis of single cavity collapse theory, by which the erosive mechanisms are (1) the liquid jet, formed by asymmertical cavity collapse[2,3] and (2) the shock wave emitted by spherical cavity collapse.[4,5] However, the calculated pressures at the specimen surface due to these mechanisms are sufficient in only a few cases to cause any macroscopic deformation or damage of the surface. Therefore enhancement effects due to concerted collapse of clusters of cavities have been proposed.[6] The evaluation of the concept of concerted collapse demands an analysis of the cluster dynamics in flow as well as in vibratory cavitation systems.[7-9] The present paper considers the dynamics of cavity cluster collapse in two cases of vibratory cavitation; (a) hemispherical cluster collapse as in moving specimen equipment and (b) cylindrical cluster collapse as in equipment with stationary specimen.

II. THE CONCEPT OF CONCERTED COLLAPSE

During the last years the idea of an effect from the concerted collapse of cavity clusters has been put forward to explain the damage capability of the cluster. Two models for the effect of concerted collapse have been proposed: one assumes that the shock waves from individual cavity collapses are superposed to form a single high-intensity damaging shock wave; the other assumes that collective collapse increases the pressure at which the last cavities collapse and that the liquid jets formed by asymmetrical collapse of the cavities close to the solid are the source of damage.

According to the first idea[6] the concerted collapse is expected to develop as follows. When the first cavities in a cluster collapse, the emitted shock waves trigger the collapse of the other cavities. The shock waves from individual cavity collapses are transmitted through the cavity cloud and are expected to catch up to form one single high-intensity shock wave, which preferably is directed towards the specimen surface. The directionality is ascribed to the increase of ambient pressure which starts at the outer cavities and initiates the collapse of the cluster. This model is based on measurements in vibratory cavitation of pressure pulses on a surface directly exposed to cavitation, and on comparison of the measured peak pressures with the corresponding values of incubation period and mass loss.[10]

In cavitation erosion studies, large-scale surface deformations (compared with the cavity diameters) are observed and the idea of an extended high-intensity shock wave as the source of erosion has its main advantage in being able to explain this large scale deformation topography (craters and undulations[11]). Meanwhile, the formation of a single regular

 0021-8979/80/094651-08$01.10

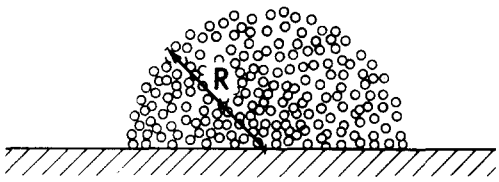

FIG. 1. Hemispherical cavity cluster at an extended solid surface.

shock wave is questionable. It is well known that each cavity emits a shock wave at collapse, but the formation of a single shock wave by collapse of the whole cluster of cavities would demand that the cavities collapse synchronously throughout the cluster. Further, even a small volume fraction of noncollapsed cavities would attenuate a shock wave very strongly. Recent experiments by Brunton[12] support this view, that no single high-intensity shock wave results from the collapse of a cavity cluster.

The other idea[8,9,13,14] is based on transfer of energy from the cavities which collapse first, to the collapse of cavities not yet collapsed. Physically, the collapse of a cavity cluster is initiated at the cluster boundary by the hydrostatic pressure in the ambient liquid, and the collapse proceeds from the boundary towards the center of the cluster. The collapse of the outer cavities creates a field of increased pressure around the remaining part of the cluster, the inward radiated energy from the collapsed cavities being transferred into collapse energy of the other cavities. Thus the damage potential of the individual cavities increases toward the center of the cluster, where the pressure increases far above the ambient pressure, and the jet velocities and the corresponding jet impact pressures become very high. This model then predicts a stronger erosion close to the center of the cavity clusters with the damaging mechanism being the jet impacts (and shock waves) from single cavity collapses. The idea of energy transfer by concerted collapse explains directly the smaller (10–100 μm) indentations[14] observed at the beginning of exposure to cavitation. The above-mentioned larger undulations are not developed until later in the erosion process. Though they may result from the integration in time and space of effects of single cavity collapses, a main drawback of this model is that it does not comprehensively explain these larger deformations. However, the focusing of the erosion to the area at the center of the cluster[13] is in direct support of this theory.

In the following, only the energy transfer model of concerted collapse is considered, because the authors of this paper do not find support of the model predicting a high-intensity shock wave. The formation of such a wave and its propagation through a cavity cluster is physically unrealistic.

III. MATHEMATICAL MODEL

In the following, the collapse of a cavity cluster is determined theoretically for the two cases: (a) collapse of a hemispherical cluster at an ultrasonic horn, which is represented by an extended solid surface, (b) collapse of an axially symmetrical cluster in the spacing between an ultrasonic horn and a stationary specimen. In both cases the pressure in the ambient liquid is assumed to rise instantaneously from the vapor pressure p_1 to a constant value p_∞ ($p_\infty \gg p_1$).

A. Hemispherical collapse

This collapse, Fig. 1, is identical to the collapse of a spherical cluster in an infinite liquid space.[9] Consider a hemispherical cluster (initially of radius R_0) of cavities in equilibrium at the pressure p_1 in a semi-infinite space. The cluster is a bubbly liquid with a volume fraction β of vaporous cavities. The sound velocity c_m inside such a cluster is given by

$$c_m^2 = p_1/\rho\beta(1-\beta), \tag{1}$$

if β is not extremely small or very near to 1 (ρ is the liquid density). If the cluster is subjected to an ambient pressure p_∞, a pressure wave with the character of a shock wave in a compressible medium is propagated into the cluster at the Mach number

$$|M_1| = (P_2/p_1)^{1/2}, \tag{2}$$

where subscripts 1 and 2 refer to conditions in front of and behind the shock front, respectively. Capital letters are used for conditions at the cluster boundary. The thickness of the shock front is of the order of $a_0/[\beta(1-M_1^{-2})]^{1/2}$, where a_0 is the initial radius of the individual cavities.

As the cavities are virtually annihilated by the shock wave ($\beta_2 = 0$), it forms the cluster boundary which moves towards the cluster center at the velocity

$$V_{sh} = c_m M_1 = \dot{R} = -[P_2/\rho\beta(1-\beta)]^{1/2}. \tag{3}$$

The velocity outside the cluster at radius r is radial, and in spherical coordinates with origin at the cluster center it becomes

$$v_r = V_r R^2/r^2 = \beta\dot{R}R^2/r^2. \tag{4}$$

From the equation of motion,

$$\frac{\partial v_r}{\partial t} + v_r\frac{\partial v_r}{\partial r} = -\frac{1}{\rho}\frac{\partial p}{\partial r},$$

the pressure distribution in the liquid is found to be

$$p = p_\infty + \rho\left(\beta\frac{2R\dot{R}^2 + R^2\ddot{R}}{r} - \beta^2\frac{R^4\dot{R}^2}{2r^4}\right), \tag{5}$$

which together with Eq. (3) gives the collapse equation for the hemispherical cluster

$$R\ddot{R} + (1 + \tfrac{1}{2}\beta)\dot{R}^2 = -p_\infty/\rho\beta, \tag{6a}$$

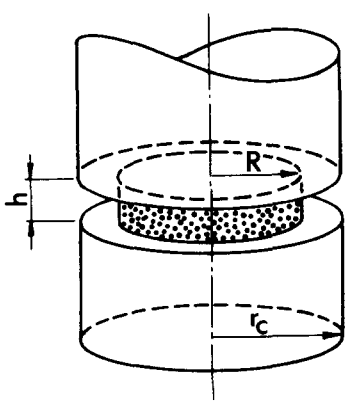

FIG. 2. Cylindrical cavity cluster in the spacing between two coaxial solid cylinders (horn and specimen).

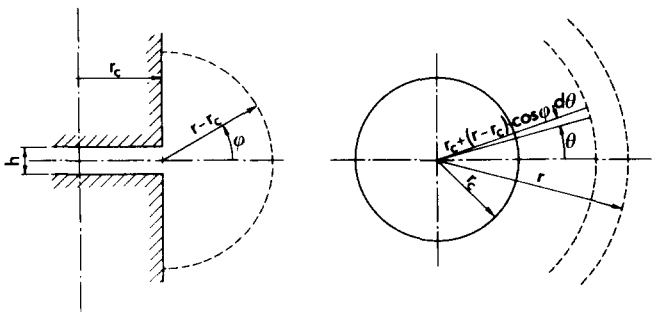

FIG. 3. Geometric parameters describing the flow regions for a stationary specimen equipment (cylindrical cavity cluster).

or in nondimensional form using

$$R^* = R/R_0 \quad \text{and} \quad t^* = (t/R_0)(p_\infty/\rho\beta)^{1/2},$$

it becomes

$$R^*\ddot{R}^* + (1+\tfrac{1}{2}\beta)\dot{R}^{*2} = -1. \tag{6b}$$

The pressure at the cluster boundary driving the collapse depends on R and is found from Eq. (3).

B. Cylindrical collapse

The case of a disc-shaped cavity cluster initially of radius R_0 between two coaxial solid cylinders (horn and specimen) of radius r_c at a distance h is shown in Fig. 2. Its collapse can be determined analogously to the collapse of a hemispherical cavity cluster. We assume that the flow between the cylinders is a two-dimensional radial flow (cylindrical collapse) which matches at $r = r_c$ to an annular sink flow in the surrounding extended liquid space. The cluster collapses with a cylindrical shock as the boundary between the cluster and the liquid. With a volume fraction β of cavities in the cluster, Eqs. (1)–(3) are as for the hemispherical case. Between the cylinders the liquid flow is radial and the velocity is

$$v_r = V_R(R/r) = \beta\dot{R}(R/r), \tag{7}$$

and at the rim of the cylindrical region $r = r_c$ the velocity becomes

$$v_{r,c} = \beta\dot{R}(R/r_c), \tag{8}$$

which of course implies $r_c > R_0$.

The equation of motion together with Eq. (7) gives

$$\frac{R\ddot{R}+\dot{R}^2}{r} - \beta\frac{(R\dot{R})^2}{r^3} = -\frac{1}{\rho\beta}\frac{\partial p}{\partial r}, \tag{9}$$

which by integration and use of Eq. (3) leads to

$$(R\ddot{R}+\dot{R}^2)\ln\frac{r_c}{R} - \dot{R}^2 + \frac{\beta}{2}\dot{R}^2\left[\left(\frac{R}{r_c}\right)^2+1\right] = -\frac{1}{\rho\beta}p_c, \tag{10}$$

where the pressure p_c at $r = r_c$ is governed by the flow outside the cylindrical region. Here the velocity v_t can be considered radial towards the rim of the cylindrical region, and uniform on toroidal surfaces in the liquid around this rim (Fig. 3).

Mass conservation demands that at any time

$$(v_r 2\pi h)_{r<r_c} = (v_t A_t)_{r>r_c}, \tag{11}$$

where A_t is the area of a toroidal surface in the outer flow at which the velocity is v_t.

The area of a toroidal surface is (see Fig. 3)

$$A_t = \int_{\phi=-\pi/2}^{\pi/2}\int_{\theta=0}^{2\pi}(r-r_c)\,d\phi\,[r_c+(r-r_c)\cos\phi\,]\,d\theta = 4\pi\,[\tfrac{1}{2}\pi(r-r_c)r_c + (r-r_c)^2]. \tag{12}$$

If we ignore the fact that a transition region exists between the cylindrical and the toroidal flow regimes and assume that they match at $r = r_c$ with continuity of velocity and pressure we can, from Eqs. (11) and (12), write

$$v_t = v_{r,c}\frac{hr_c}{(r-r_c)[2r+r_c(\pi-2)]}, \tag{13}$$

from which

$$v_t = v_{r,c} \text{ at } r-r_c = \tfrac{1}{4}\pi r_c[-1+(1+8h/\pi^2 r_c)^{1/2}] \simeq h/\pi \text{ for } h/r_c \ll \pi^2/8. \tag{14}$$

For the toroidal flow, Eqs. (8) and (13) together with the equation of motion give

$$\frac{h}{(r-r_c)[2r+r_c(\pi-2)]}\times\left\{R\ddot{R}+\dot{R}^2-(R\dot{R})^2\beta\frac{h(4r+r_c(\pi-4))}{(r-r_c)^2[2r+r_c(\pi-2)]^2}\right\} = -\frac{1}{\rho\beta}\frac{\partial p}{\partial r}, \tag{15}$$

which by integration from the lower limit of r, Eq. (14), to $r\to\infty$, leads to

$$(R\ddot{R}+\dot{R}^2)\pi\delta\ln\frac{1+2\delta}{2\delta} - \beta\dot{R}^2\frac{R^2}{h^2}\pi^4\delta^4\left(\frac{1-4\delta}{2\delta^2}\right) = \frac{1}{\rho\beta}(p_\infty - p_c), \tag{16}$$

where

$$\delta = h/\pi^2 r_c \ll \tfrac{1}{8}.$$

Equations (10) and (16) give the equation of motion for the cylindrical collapse of a cavity cluster,

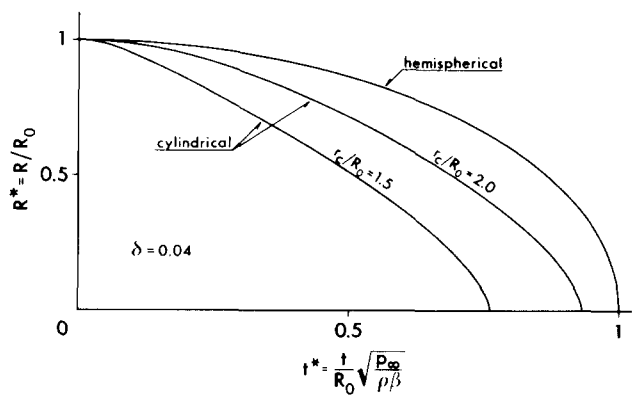

FIG. 4. The cavity cluster radius R during collapse as a function of time (in nondimensional form) for a hemispherical cluster and for two cases of a cylindrical cluster ($\beta <<< 1$ in all the cases).

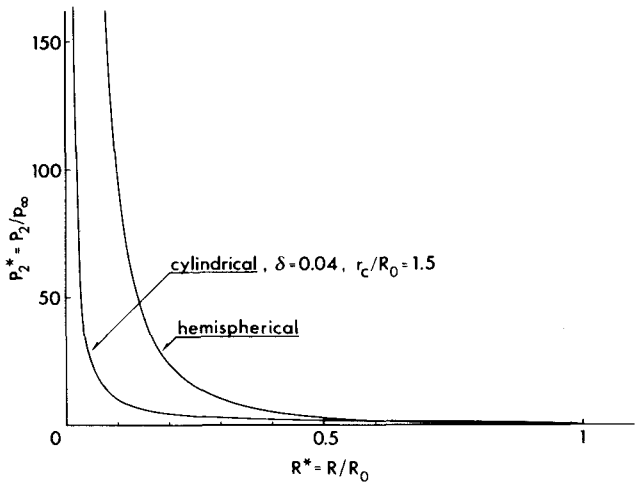

FIG. 5. The pressure P_2 at the cluster boundary as a function of the cluster radius R (in nondimensional form) during collapse of a hemispherical and a cylindrical cluster ($\beta <<< 1$ in both cases).

$$(R\ddot{R} + \dot{R}^2)\left(\ln\frac{r_c}{R} - \pi\delta\ \ln\frac{1+2\delta}{2\delta}\right) - \dot{R}^2 + \beta\dot{R}^2 \times [\tfrac{1}{2} + (R/r_c)^2(1-2\delta)] = -p_\infty/\rho\beta, \tag{17a}$$

or in nondimensional form

$$(R^*\ddot{R}^* + \dot{R}^{*2})\left(\ln\frac{r_c^*}{R^*} - \pi\delta\ \ln\frac{1+2\delta}{2\delta}\right) - \dot{R}^{*2} + \beta\dot{R}^{*2}\,[\tfrac{1}{2} + (R^*/r_c^*)^2(1-2\delta)] = -1 \tag{17b}$$

[cf. Eq. (6) for hemispherical collapse].

The largest pressure is obtained at the boundary of the collapsing cluster and it is a function of R given by Eq. (3). In both of the above cases the influence of the oscillations of the ultrasonic horn itself on the collapse of the cluster is not taken into consideration.

In the above theory a homogeneous distribution of cavities in the cluster has been assumed, and the thickness of the shock front at the cluster boundary has been ignored. This means that when the cluster radius approaches the mean cavity spacing Δl the theory becomes invalid. For spherical cavities this distance is

$$\Delta l = a_0 \cdot (4\pi/3\beta)^{1/3}. \tag{18}$$

It should be mentioned that when the individual cavities collapse, the potential energy in the system represented by the initial cavities is converted into kinetic energy of the liquid. This energy is directed towards the cluster, but when a cavity is annihilated, a shock wave is emitted which carries part of the energy away from the cluster. As a result, the kinetic energy of the liquid surrounding the cluster vanishes when the cluster radius vanishes, and consequently no single high-intensity shock wave can be expected to be emitted at the end of the cluster collapse, but during the collapse a shock wave is emitted from each of the individual cavities. The photographs by Brunton[12] support this.

IV. NUMERICAL EXAMPLES

It is seen from the collapse Eqs. (6) and (17) that the volume fraction β of cavities in the cluster, the hydrostatic

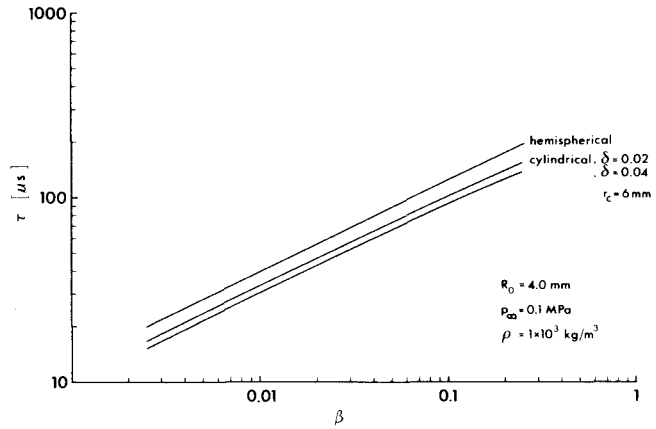

FIG. 6. The total collapse time τ as a function of the volume fraction β of cavities for a hemispherical cluster and for two cases of a cylindrical cluster.

prsesure p_∞ in the ambient liquid, and the density ρ of the liquid are the principal parameters. Apart from a second-order influence of β, the total collapse time τ is proportional to $(\rho\beta/p_\infty)^{1/2}$.

In their general form the second-order differential Eqs. (6) and (17) are solved numerically, i.e., the collapses are numerically simulated from the initial boundary conditions. These are at the time $t = 0$, cluster radius R_0 equal to the experimentally observed maximum cluster radius, and the velocity of the cluster boundary $\dot{R}_0 = 0$. The parameters r_c and δ [in Eq. (17)] are cavitation equipment constants and R_0 and β depend on the horn amplitude and the frequency. The method adopted for the successive numerical solutions is a fourth-order Runge-Kutta method[15] and the equations

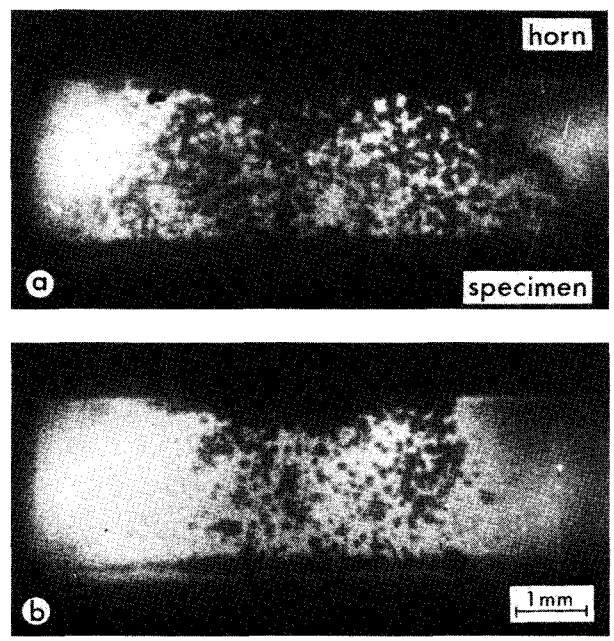

FIG. 7. Cavity clusters in an ultrasonic cavitation equipment with a stationary specimen. The pictures are taken with transmitted light through the cavity clusters. (a) Fully developed cluster and (b) partially collapsed cluster. Frequency of the horn vibrations $f = 20$ kHz, horn amplitude $A = 2.5$ μm, horn-specimen distance $h = 2.4$ mm and ambient pressure $p_\infty = 0.10$ MPa.

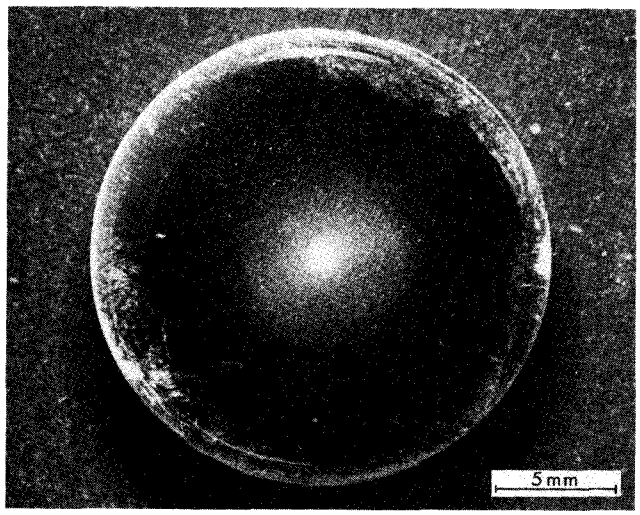

FIG. 8. Aluminum specimen exposed to ultrasonic cavitation for 60 s. The surface is strongly distorted only at the center and the damage decreases rapidly in radial direction. $f = 20$ kHz, $A = 3.7\ \mu$m, $h = 1.0$ mm and $p_\infty = 0.10$ MPa.

are solved in nondimensional forms with the aid of a programmable calculator. The step length between the successive numerical solutions is chosen for each step to give the solution as accurate as possible.

By hemispherical collapse p_∞, ρ and β are the only parameters, and for $\beta \lll 1$ the solution of the nondimensional Eq. (6b) is simply

$$R^{*2} = 1 - t^{*2}$$

(see Fig. 4). The velocity of the cluster boundary is seen to approach infinity in the final stage of collapse, where the cluster radius vanishes at $t^* = 1$. Consequently, according to Eq. (3) the pressure in the liquid at the cluster boundary also approaches infinity (Fig. 5). The full solution of Eq. (6) shows that the nondimensional time for total hemispherical cluster collapse τ^* changes from 1 to 0.98 if β changes from ~ 0 to 0.25, and the dependence is nearly linear.

For cylindrical cluster collapse Eq. (17) with $\beta \lll 1$, solutions are shown in Fig. 4 for $\delta = 0.04$ ($r_c = 6.0$ mm, $h = 2.4$ mm) at values of $r_c/R_0 = 1.5$ and 2.0. Here the final collapse velocities also approach infinity, but at corresponding collapse stages they are lower than for the case of hemispherical collapse. As in the hemispherical case, τ^* is reduced at increasing β (but less than 10% at $\beta = 0.25$). The pressure at the cluster boundary is shown in Fig. 5 for $\delta = 0.04$, $r_c/R_0 = 1.5$ From an erosion point of view, it is the absolute collapse pressures P_2 and the total collapse time τ for the cluster which are of interest. These pressures are readily obtained from Fig. 5 ($\beta \lll 1$) as $P_2 = P_2^* p_\infty$. In Fig. 6 the total collapse time τ as a function of β for a cavity cluster of initial radius $R_0 = 4.0$ mm is shown for hemispherical collapse, and for cylindrical collapse at $\delta = 0.04$ and 0.02 with $r_c = 6.0$ mm, $p_\infty = 0.1$ MPa, and $\rho = 10^3$ kg/m^3. It is seen that in all the cases τ is almost proportional to $\sqrt{\beta}$.

V. EXPERIMENTAL RESULTS

A. Observations of cluster collapses

The life cycle of a cavity cluster in a 10-kHz acoustic field generated in a water filled cylindrical beaker by means of a ring transducer was recorded photographically by Ellis.[16] Hemispherical clusters were formed and collapsed in each cycle of the acoustic field on the axis at the bottom of the beaker, where the maximum pressure amplitude occurred. Ellis used a photoelastic material as bottom in the beaker. At the center of the cluster he observed a strong pressure pulse when the last cavity in the cluster was collapsed immediately adjacent to the surface of the photoelastic material. The collapse of the individual cavities was found to be nonspherical. Ellis's photographs show that during the period of growth the cavities grow simultaneously in the whole region occupied by the cluster, but the cluster collapses from its outer boundary, and the cavities at the center of symmetry at the solid surface are the last ones to collapse, as described in the present theory. The collapse time for a cluster of radius $R_0 = 1.5$ mm is found from the photographs to be $\tau \simeq 40\ \mu$s, and the volume fraction of the cavities can be estimated from these photographs to be $\beta \cong 0.1$ (experiments carried out at atmospheric pressure). The collapse time computed from the present theory on the basis of these data agrees with the measured value of τ.

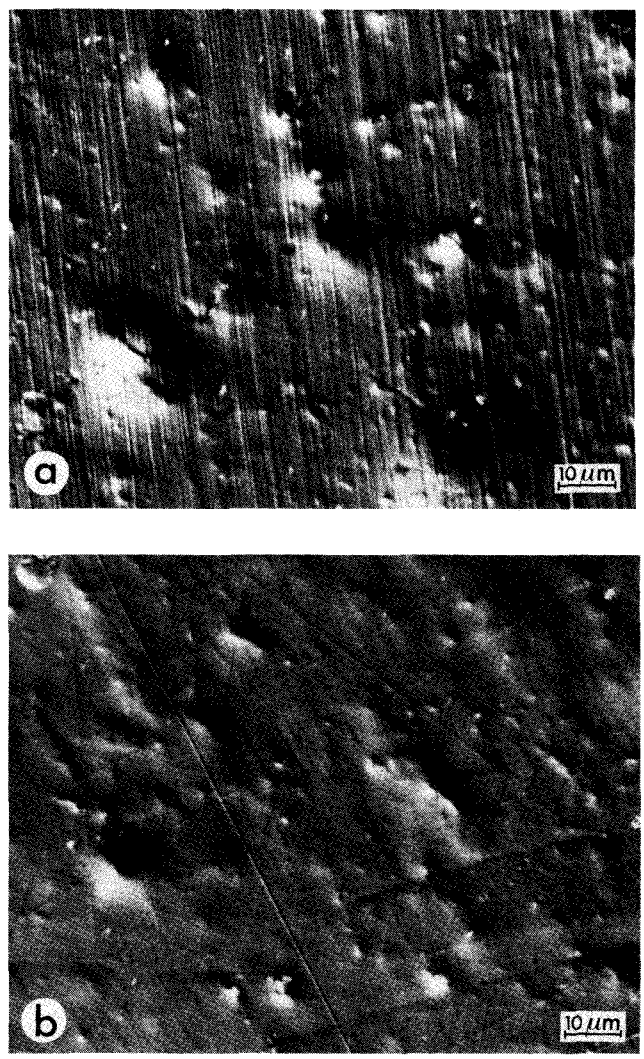

FIG. 9. Initial stage cavitation erosion with indentations in the surface, (a) aluminum and (b) austenitic stainless steel.

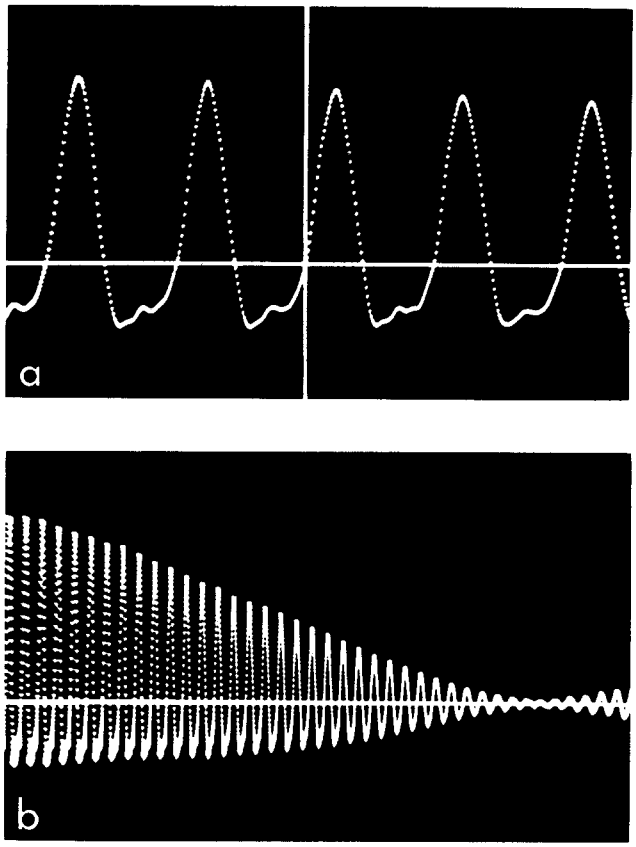

FIG. 10. The pressure variations (frequency 20 kHz) at the container wall without absorbing lining. (a) The pressure variations at cavitation and (b) their attenuation after switch off. (The horizontal line represents the mean pressure).

An analogous life cycle is found by Hansson and Mørch[13,14] for the almost cylindrical cavity clusters generated between an oscillating cylindrical horn and a stationary specimen submerged in water (20 °C) in a container with sound absorbing walls. In these experiments the horn was vibrated at 20 kHz with amplitdues of 3–4 μm. At $p_\infty = 0.1$ MPa it was found that total collapse was not achieved in each cycle, but it could stretch over 2–3 cycles. Onset of cavitation was found to occur at amplitudes of the horn tip slightly less than 2 μm. It is seen in Fig. 7 that the cluster collapses essentially radially. Towards the end of the collapse, however, the cavities tend to collapse earlier at the horn than at the specimen. This is attributed to the pressure wave from the oscillating horn, which is superimposed on the radial wave set up by the ambient pressure. From the photographs the volume fraction of the cavities is estimated to be $\beta \simeq 0.01$ and with $R_0 \simeq 4$ mm, $p_\infty = 0.1$ MPa, a collapse time of 30 μs is calculated (Fig. 4). With the period of oscillation of the horn being 50 μs, collapse of the cluster in each cycle demands that the collapse time is less than 25 μs. Therefore, according to this calculation, it is not surprising that collapse does not take place in each cycle in these experiments.

B. Observations of surface deformations

In the ultrasonic cavitation apparatus with stationary specimen, the erosive effects of cavitation was investigated using polished specimens of aluminum and austenitic stainless steel. Typically, these specimens were fixed 2 mm from the horn. The cavitation exposure time was in the range 1–60 s. With amplitudes of oscillation of the horn of the order of 3–4 μm (ambient pressure $p_\infty = 0.1$–0.2 MPa), only initial stage erosion occurred, characterized by the initial surface deformations of the incubation period, but no mass loss. It is characteristic that the erosion pattern is centered at the cluster center and that the erosion in all cases increases strongly towards the center, where an area of diameter 1–2 mm is very much stronger eroded than the surrounding area (Fig. 8). In stainless steel the surrounding area was not visibly eroded at all, but in aluminum surface deformations occurred over a larger area. At the shortest exposure time the surface damage appears as isolated, shallow indentations even at the center. At the longer exposure times the indentations close to the center overlap and merge into a more heavily distorted surface, while they remain separated towards the rim of the eroded area. The indentations are of diameter up to about 25 μm and depth about 1 μm, and in general, smaller in stainless steel than in aluminum (Fig. 9).

VI. DISCUSSION

A result of the present theory is that the collapse time for a cavity cluster is of the order of $\tau = R_0(\rho\beta/p_\infty)^{1/2}$ for cylindrical, as well as for hemispherical collapse, which seems to agree with the experimental results.

For the understanding of the cavitation erosion process, however, the most important result is that a cavity cluster collapses from its outer boundary towards the center and that the pressure, at which the individual cavities collapse, increases sharply towards the center (Fig. 5). Consequently, the collapse velocities of the cavities at the center of the cluster are much higher than those obtained in the outer part of the cluster where the pressure is not very much different from the ambient pressure. Therefore the central cavities are much more erosive than the other cavities in the cluster. This is confirmed by Ellis's cluster collapse photographs[16] as well as by the erosion patterns observed in the present experiments where the cluster collapse is centered at the specimen surface. Here the individual cavities will collapse nonspherically, forming jets towards the solid surface. If a cavity touches the surface the jet impact is direct, otherwise the jet impact pressure wave passes through a thin liquid layer before it reaches the solid. It means that only favorably positioned cavities (cavities very close to the solid surface) and preferably those at the cluster center are able to cause damage. The indentations characteristic of the very first damage correspond reasonably well in mean diameter (< 25 μm) to the expected damageable pressure distribution.

It has been assumed in this theory that the ambient pressure changes discontinuously from p_1 to a constant value $p_\infty \gg p_1$, when the collapse of the cluster is initiated. Actually, the ambient pressure is at a constant level all the time, and throughout the liquid the pressure fluctuations are determined by the liquid motion set up by the motion of the horn (oscillator) and of the cluster under the influence of the ambient pressure together with possible reflected waves in the container.

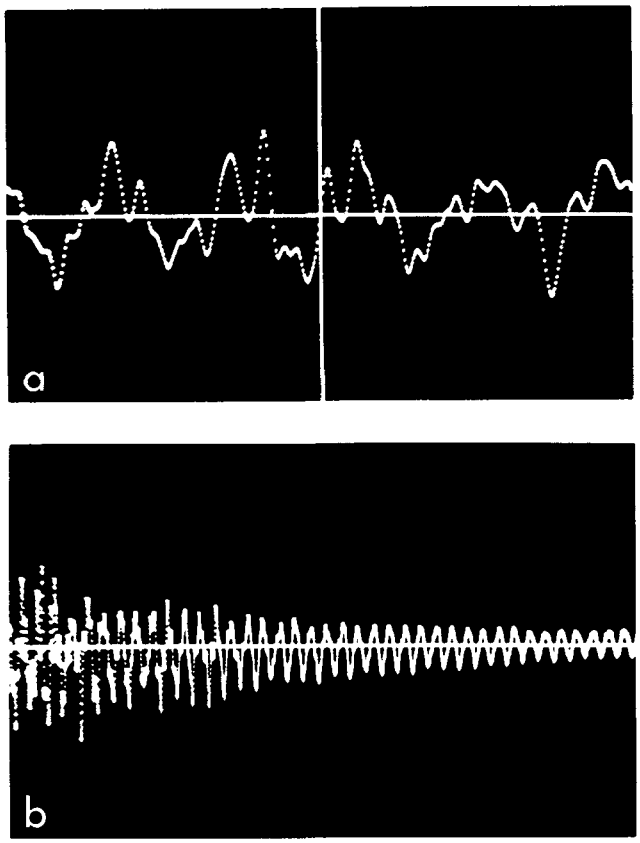

FIG. 11. The pressure variations (frequency 20 kHz) at the container wall with absorbing lining. (a) The pressure variations at cavitation and (b) their attenuation after switch off. (The horizontal line represents the mean pressure). The pressure transducer signal is amplified by a factor of 10 compared with Fig. 10.

A complete analysis of this model must be based on the pressure wave emitted from the horn. The cluster itself influences the wave and such an analysis also raises the problems of the inception and growth of the cluster. These are far more complicated than the collapse problem presented here. If the oscillating horn is considered at amplitudes so low that cavitation does not occur, the condition at the horn corresponds to the nearfield of a simple sound source. Thus, maximum pressure occurs when the horn surface passes maximum displacement towards the horn and minimum pressure when it passes maximum displacement towards the liquid. The liquid will then experience a negative pressure just after the displacement has passed the zero position, in the half-cycle with movement towards the liquid, until just before the displacement again passes the zero position on its movement towards the horn. At cavitating horn amplitudes, the cavity nucleation will occur in the first quarter-cycle of the half-cycle with a negative pressure and beyond this point the pressure will be almost equal to the vapor pressure and the cavities will grow until the ambient pressure reverses the flow in the liquid towards the horn. Then, when the pressure starts to be positive again the collapse will proceed as described earlier in the present paper. If the cluster has not collapsed when the surface of the horn becomes displaced towards the horn from its zero position, its deceleration will give rise to a pressure wave at the horn cluster interface which also will contribute to a faster cluster collapse. For very large amplitudes this pressure wave may be important even when compared with the collapse wave described in this paper and the combined waves give rise to other erosion patterns (area or ring shaped) than the centered one described here.

The pressure wave emitted by the vibrations of the horn and by the collapsing clusters spread radially in the container. The waves are reflected at the container wall (usually a glass beaker) if no precautions are taken to absorb them. Thus a pattern of standing waves is built up in the container and in the case of radial symmetry the amplitude increases towards the central axis. Measurements of the pressure variations at the container wall have been made with absorbing lining on the container wall (Fig. 11), as well as without (Fig. 10). The attenuation of the waves, after switch off of the driving power to the ultrasonic transducer, is also seen in these figures. It is seen that the positive pressure half-cycle is much larger for a container without lining than with lining, which is a consequence of the reflected waves. For a nonabsorbing cylindrically symmetrical container (e.g., a glass beaker) this means that the effective collapse pressure of the cluster is highly increased. In our experimental equipment the pressure variations are estimated to be higher by a factor of approximately 20 at the cluster position than at the container wall. Therefore, a much shorter total cluster collapse time τ will be realistic when reflections are permitted than the one estimated from the ambient pressure alone. In most experimental setups this will be the case, and then the clusters may collapse in each cycle of the horn vibrations.

In a more detailed discussion, some other factors influencing the theoretical results should be mentioned. One of these is that the theory presented here does not include the shock waves produced when each individual cavity collapses. The energy of these shock waves is to some extent transported into the cluster and intensifies the collapse.[9] Another important factor is that deviations from the perfect hemispherical and cylindrical cluster configurations cause defocusing of the pressure wave. Therefore, a smaller pressure increase is obtained during the collapse. However, towards the end of the cluster collapse, where defocusing is most important, the nonvanishing spacing between the cavities [Eq. (18)] already limits the applicability of the theory. It is reasonable to assume that the defocusing will prevent that the pressure in the implosion wave set up by the collapse of the cluster increases significantly beyond that obtained from the theory at a cluster radius of order as the mean cavity spacing. We can estimate the maximum pressures as follows: For $\beta = 0.01$ and $a_0 = 50\,\mu$m, Eq. (18) gives $\Delta l = 0.4$ mm. Thus, if $R_0 = 4.0$ mm, the lower limiting value of $R^* = 0.1$, where $P_2^* \simeq 10$ and 100 in the cylindrical and hemispherical collapse cases, respectively (given in Fig. 5). At ambient pressures of 0.1 MPa, it is evident that the pressure at the cluster boundary is far from reaching a level which is damaging to solids even at the end of the cluster collapse, but the pressure at which the individual cavities collapse is significantly increased towards the center of the cluster and the erosive effect of the wall-near cavities is cor-

respondingly increased. This is clearly demonstrated by the initial stage erosion patterns obtained in the ultrasonic cavitation apparatus with stationary specimen (cylindrical collapse) Fig. 8, in which the initial cluster radius $R_0 \simeq 4$ mm, while the erosion is concentrated within a central area of diameter only 1 mm.

VII. SUMMARY

The present paper shows that the energy transfer model of concerted collapse is physically realistic and leads to agreement between theoretical and experimental results. The concerted collapse makes the central cavities in a cavity cluster highly damaging due to the strong increase of the local hydrostatic pressure. The cavitation erosion can be ascribed primarily to the collapse of the individual cavities in this center region, intensified by the concerted collapse of the other cavities.

The total collapse time of a cavity cluster is theoretically estimated to be $R_0(\rho\beta/p_\infty)^{1/2}$, which agrees well with experimental results.

The importance of standing waves in the container is shown and it is concluded that in vibratory cavitation erosion equipment such waves strongly influence the life cycle of the clusters.

[1] *G32-72, Annual Book of ASTM Standards* (American Society for Testing Materials, Philadelphia, 1979), Vol. 10, p. 822.
[2] A. Kornfeld and L. Suvorov, J. Appl. Phys. **15**, 495 (1944).
[3] M. S. Plesset and R. B. Chapman, J. Fluid Mech. **47**, 283 (1971).
[4] F. R. Gilmore, Report 26-4, California Institute of Technology, Hydrodyn. Lab. (1952) (unpublished).
[5] R. Hickling and M. S. Plesset, Phys. Fluids **7**, 7 (1964).
[6] B. Vyas and C. M. Preece, Am. Soc. Test. Mater., Spec. Tech. Publ. **567**, 77 (1974).
[7] L. van Wijngaarden, *Proc. 11th International Congress of Applied Mechanics, Munich, 1964*, **854** (Springer, Berlin, 1966).
[8] K. A. Mørch, *Proc. Acoustic Cavitation Meeting, Poole, Dorset* (Institute of Acoustics, London, 1977), p. 62.
[9] K. A. Mørch, *Springer Series in Electrophysics* (Springer, Berlin, 1980), Vol. 4, p. 95.
[10] B. Vyas and C. M. Preece, J. Appl. Phys. **47**, 5133 (1976).
[11] V. Vyas and C. M. Preece, Met. Trans. Ser. A **8**, 915 (1977).
[12] J. H. Brunton, *Proceedings of the 5th International Conference on Erosion by Solid and Liquid Impact, 1979* (Cavendish Laboratory, Cambridge, United Kingdom, 1979), paper 59, pp. 1–7.
[13] I. Hansson and K. A. Mørch, *Proceedings of the Ultrasonics International Conference, Graz, 1979,* (IPC Science and Technology, United Kingdom, 1979), p. 221.
[14] I. Hansson and K. A. Mørch, *Proceedings of the 5th International Conference on Erosion by Solid and Liquid Impact, 1979,* (Cavendish Lab., Cambridge, United Kingdom, 1979), paper 60, pp. 1–9.
[15] C. Fröberg, *Introduction to Numerical Analysis* (Addison-Wesley, London, 1970).
[16] A. T. Ellis, *Cavitation in Hydrodynamics, Proceedings from National Physics Laboratories Symposium, 1955* (Her Majesty's Stationery Office, London, 1956).